

# Effect of carbon content on the Hall-Petch parameter in cold drawn pearlitic steel wires

WON JONG NAM

*Kookmin University, Seoul, 136-702, Korea*

*E-mail: wjnam@kmu.kookmin.ac.kr*

CHUL MIN BAE

*POSCO Technical Research Laboratories, Pohang, 790-785, Korea*

CHONG SOO LEE

*Center for Advanced Aerospace Materials, Pohang University of Science and Technology, Pohang, 790-784, Korea*

The effect of the carbon content on the Hall-Petch parameter has been investigated for fully pearlitic steels with the carbon range of 0.52–0.92 wt%. The increase of the carbon content in pearlitic steels enhances tensile strength and hardening rate of cold drawn pearlitic steels by the refinement of the initial interlamellar spacing and the increase of the Hall-Petch parameter. The Hall-Petch parameter is not influenced by the initial interlamellar spacing of pearlite although refining the initial interlamellar spacing increases tensile strength and hardening rate during wire drawing. However, the carbon content in cold drawn pearlitic steels significantly affects the magnitude of the Hall-Petch parameter. The magnitude of the Hall-Petch parameter,  $k$ , is expressed as a function of the volume fraction of cementite ( $V_c$ , i.e. the carbon content);  $k = \text{constant} \cdot V_c^{1/2} \cdot (1 - V_c)$ , which shows a good agreement between experimental and calculated values. © 2002 Kluwer Academic Publishers

## 1. Introduction

It has been generally accepted that strength of pearlitic steels can be predicted by the Hall-Petch relationship [1, 2].

$$\sigma = \sigma_0 + K \cdot \lambda^{-1/2} \quad (1)$$

where  $\sigma$  is the stress,  $\sigma_0$  is the friction stress,  $K$  is the Hall-Petch constant and  $\lambda$  is the interlamellar spacing of pearlitic steels. Especially, the modified form of the Hall-Petch relationship proposed by Embury and Fisher [3] has been widely used in the steel wire industry in estimating strength of cold drawn eutectoid steels, due to its accuracy and convenience of measuring the initial interlamellar spacing and drawing strain;

$$\sigma = \sigma_0 + [k/(2\lambda_0)^{1/2}] \cdot \exp(\varepsilon/4) \quad (2)$$

where  $\varepsilon$  is the true drawing strain,  $\lambda_0$  is the initial interlamellar spacing and  $k$  is the Hall-Petch parameter. The magnitudes of  $k$  and  $\lambda_0$  in the Equation 2 are equivalent to  $\sqrt{2} \cdot K$  and  $\lambda \cdot \exp(\varepsilon/2)$  in the Equation 1, respectively [4, 5].

Recently, development of high strength steels manufactured by the cold drawing process has become an important subject in the steel wire industry. The Equation 2 shows three ways to increase strength of cold drawn pearlitic steels; (a) the increase of the Hall-Petch parameter, (b) the reduction of the initial interlamellar

spacing and (c) the increase of the drawing strain. So far, most works have focused on the investigation on (b) and (c) which are related to each other [5–7]. In pearlitic steels with fixed carbon content, the interlamellar spacing is considered as the most suitable factor to determine strength of steels. However, when carbon contents are varied in pearlitic steels, the interlamellar spacing is no more a single proper variable since strength is significantly affected by the variation of the volume fraction of cementite. Thus, it seems more reasonable to investigate  $k$  in relation to the variation of the carbon content since  $k$  would reflect the effect of the carbon content through the microstructural variation. Recent work on  $k$  [8] has shown that  $k$  increases with the carbon content without showing any detailed analysis.

Previous investigations [9, 10] have reported that volume fraction of pro-eutectoid ferrite in hypo-eutectoid steels, can be reduced by controlling several factors related to transformation kinetics, such as austenitizing temperatures and transformation temperatures, which results in a nearly fully pearlitic microstructure, i.e., the pearlite without pro-eutectoid ferrite (less than 2%). Accordingly, the deficiency of carbon contents in the pearlite region induces the formation of ‘degenerate pearlite’, i.e. non-lamellar pearlite, which differs in morphology and volume fraction of cementite from eutectoid pearlite. The degeneracy of pearlite increases as the carbon content is decreased. However, during wire drawing the main features of the microstructural

changes are a progressive alignment of lamellar cementite along the drawing axis, a reduction of interlamellar spacing and a thinning of lamellar cementite [3, 4, 7, 11–17]. Accordingly, lamellar cementite is plastically deformed into the elongated shape along the drawing direction during wire drawing. Subsequently, the fibrous shaped cementite in cold drawn hypo-eutectoid steels can be considered similar to that of cold drawn eutectoid steels. Thus, fully pearlitic microstructures with various carbon contents from hypo-eutectoid to hyper-eutectoid cold drawn steels would be useful in investigating the influences of the carbon content on the Hall-Petch parameter.

In view of the foregoing, it is attempted in this study to investigate the variation of the Hall-Petch parameter,  $k$  with the carbon content (0.52–0.92 wt%) in cold drawn pearlitic steels, and to establish a quantitative relationship between  $k$  and the carbon content.

## 2. Experimental procedures

Steels used in this study were Stelmor-cooled wire rods with chemical compositions of 0.52–0.92% C, 0.2% Si, 0.5% Mn (in wt%) and the balance Fe (Table I). The wire rods with 5.5 mm in a diameter were austenitized at 1223 K for 10 min. followed by quenching in a salt bath in the temperature range of 823 K–923 K. In 0.52% C steel, the presence of pro-eutectoid ferrite was occasionally found. Since volume fraction of pro-eutectoid ferrite, however, is found to be less than 2%, the contribution of pro-eutectoid ferrite on mechanical properties is assumed insignificant in this study. The rod was, then, pickled and successively cold drawn with the average reduction per pass of 25%, at a relatively low drawing speed of 3 m/min, to avoid the dynamic strain aging effect. Tensile specimens were taken after each pass and tensile tests were performed at room temperature with a constant speed of displacement. An initial strain rate was  $8.3 \times 10^{-4}$ /s.

For a detailed understanding of the microstructures after the heat-treatment, scanning electron microscope (SEM) was used. The initial interlamellar spacing was estimated by a linear intercept method in SEM micrographs with the magnification of 10000. Specimens for TEM observation were prepared by jet polishing in a mixture solution of 5% perchloric acid and 95% acetic glacial acid.

## 3. Results

### 3.1. Microstructures

When the fully pearlitic microstructure is obtained in steel A containing 0.52% C by austenitizing at 1223 K followed by an isothermal transformation at 853 K, the carbon content of the pearlite region remains as 0.52%.

TABLE I Chemical composition of steels

	C	Mn	Si	S	P
Steel A	0.52	0.49	0.19	0.006	0.017
Steel B	0.67	0.49	0.18	0.006	0.010
Steel C	0.82	0.49	0.22	0.004	0.004
Steel D	0.92	0.49	0.22	0.004	0.011

All values are in wt%.

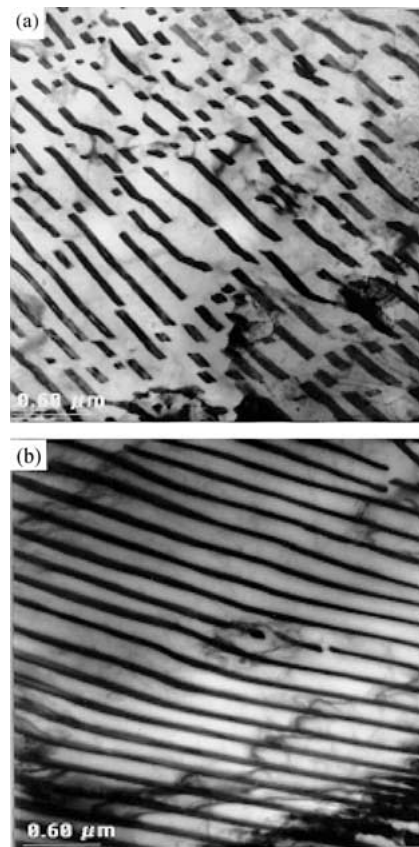


Figure 1 TEM microstructures showing different pearlite morphology in (a) steel A and (b) steel C transformed at 853 K.

Therefore, the carbon content of 0.52% in the pearlite region induces the degenerate pearlite. It is of interest to note that morphology of cementite in hyper-eutectoid or eutectoid steels is a type of continuous plates while that of hypo-eutectoid steel is a type of discrete ones (Fig. 1). Consequently, fully pearlitic microstructure of medium carbon steel exhibits different cementite volume fraction and morphology compared to that of high carbon steel.

Fig. 2 shows microstructures of a longitudinal cross-section of the drawn wires of steel A (0.52% C) with the increase of drawing strain. The morphological change of degenerate pearlite during wire drawing is similar to that of eutectoid steels in previous investigations [11–17]; cementite lamellae that are initially randomly oriented become progressively aligned along the drawing axis with the increase of drawing strain. The cementite lamellae oriented favorably or parallel to the drawing axis are plastically deformed and thinned to a fibrous shape, while those oriented unfavorably or vertically to the drawing axis are bent and/or kinked. However, with the increase of drawing strains, the bent and/or kinked cementite lamellae are also plastically deformed and aligned parallel to the drawing axis. Thus, after the drawing of  $\epsilon = 2.06$  in Fig. 2c, most cementite lamellae are aligned along the drawing axis, and the kinked and/or bent cementite lamellae are rarely found. As shown in Fig. 2d, further straining results in the alignment of virtually all the fibrous shaped cementite lamellae along the drawing axis.

Microstructures of a transverse section of the drawn pearlitic steel wires (steel C3) are illustrated in Fig. 3.

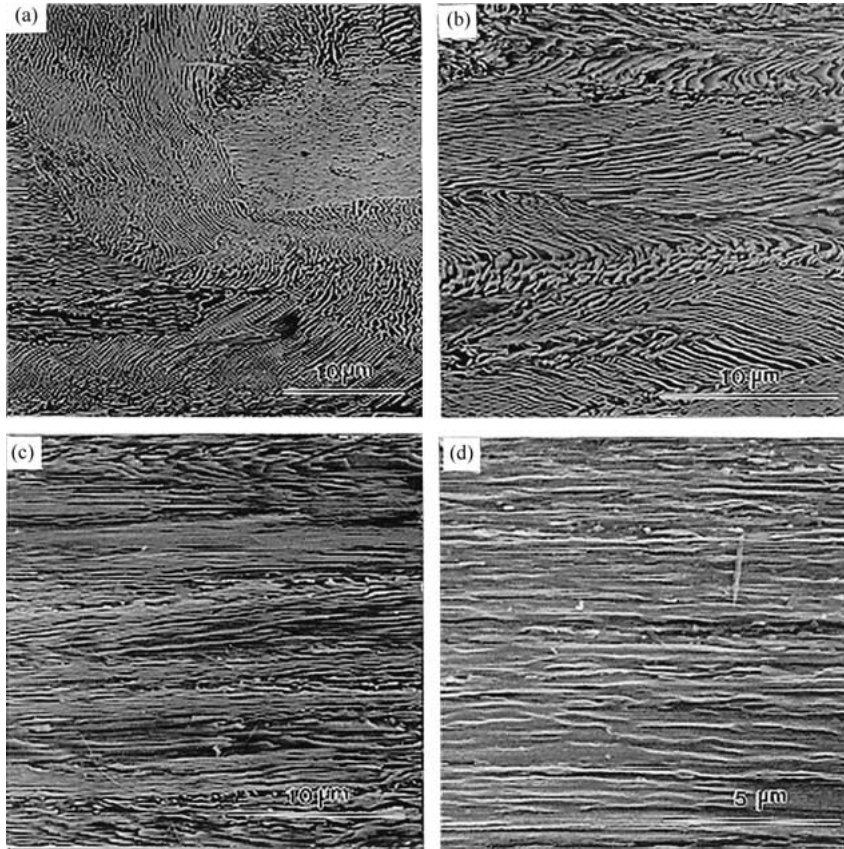


Figure 2 Microstructures of a longitudinal cross-section of cold drawn steel A: (a)  $\varepsilon = 0.61$ ; (b)  $\varepsilon = 1.19$ ; (c)  $\varepsilon = 2.06$ ; (d)  $\varepsilon = 2.63$ .

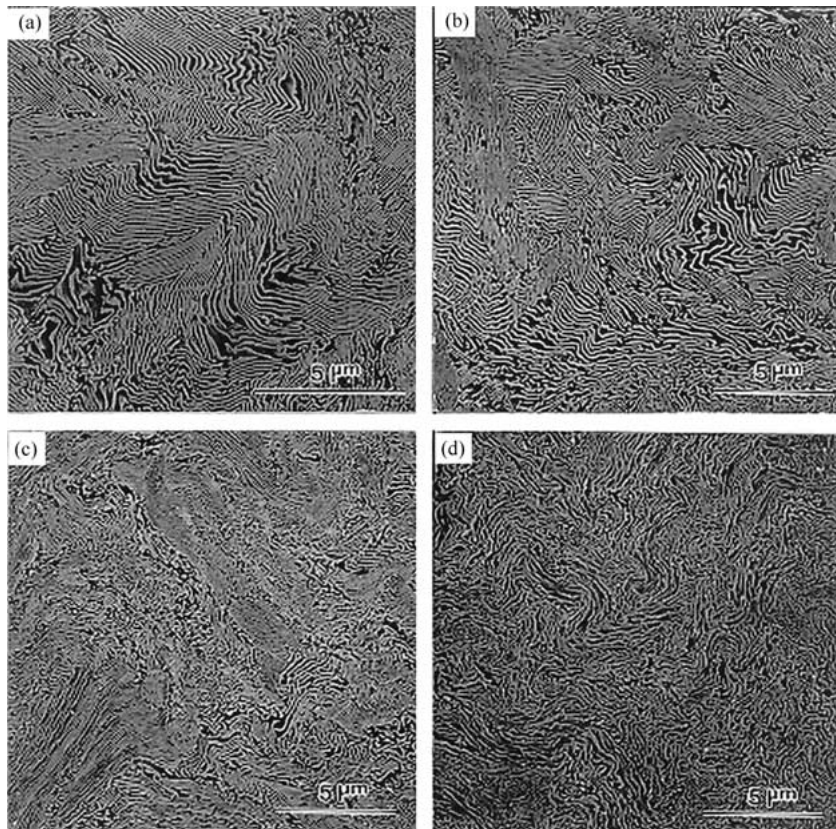


Figure 3 Microstructures of a transverse cross-section of cold drawn steel C3: (a)  $\varepsilon = 0.61$ ; (b)  $\varepsilon = 1.19$ ; (c)  $\varepsilon = 2.06$ ; (d)  $\varepsilon = 2.63$ .

Pearlite colonies exhibit a wavy or intercurled microstructure that is typical in the drawn wires with bcc structure. In addition, the variation of microstructures in Fig. 3a–d indicates that the degree of the intercurling becomes severer with increasing drawing strain so as to

maintain a compatibility between neighboring colonies [18]. This intercurled microstructure is attributed to the deformation under plane strain condition that is associated with the formation of  $\langle 110 \rangle$  texture in ferrite during the drawing.

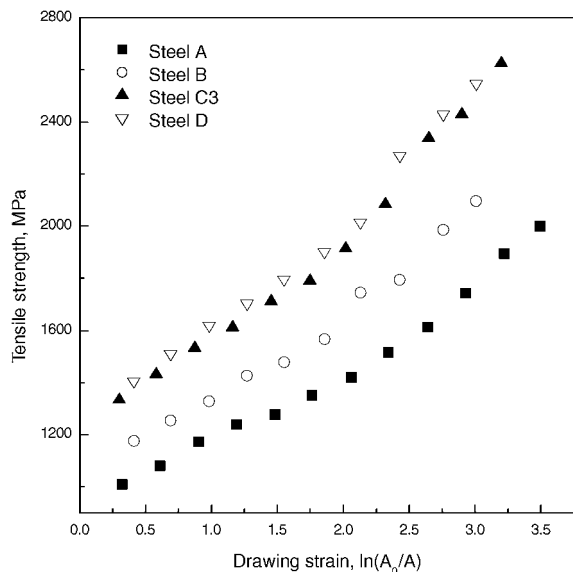


Figure 4 The variation of tensile strength of the cold drawn steel wires as a function of drawing strain.

### 3.2. Mechanical properties

Microstructural changes discussed above are closely related to the variations of mechanical properties of the drawn wires. Fig. 4 shows the variation of tensile strength of the drawn wires as a function of drawing strain, in which tensile strength increases continuously with drawing strain. The hardening behavior of pearlitic steels can be reasonably explained with the Hall-Petch relation. With the increase of drawing strain, interlamellar spacing is reduced, resulting in the increase of tensile strength. The rapid increase of tensile strength after about  $\varepsilon = 2.0$  is attributed to work hardening of the completely aligned lamellae.

It is also noted in Fig. 4 that steels containing higher carbon content (steel C3 and steel D) apparently show higher tensile strength and hardening rate during wire drawing. The higher hardening rate in steel C3 and steel D at a fixed strain can be explained as the increase of the Hall-Petch parameter and/or the refinement of the initial interlamellar spacing in steels. But, it is not clear which factor plays a more important role in enhancing tensile strength and hardening rate. It is also of interest to investigate whether the Hall-Petch parameter has been evidently increased in high carbon steels.

To understand better the sole effect of the initial interlamellar spacing on mechanical properties, the initial interlamellar spacing of steel C has been varied by transforming the specimens at different temperatures. Since the carbon content is fixed in steel C, the variation of mechanical properties will not be associated with the carbon content. Fig. 5a shows the plot of tensile strength of steel C with different initial interlamellar spacing versus strain parameter,  $\exp(\varepsilon/4)$ . Tensile strength increases linearly with the strain parameter. Also, it is noticed that hardening rate (the slope of the lines) increases as the initial interlamellar spacing decreases. It is interesting to observe that the Hall-Petch parameter does not vary significantly, as shown in Table II and Fig. 6, with the variation of the initial interlamellar spacing, representing about  $590 \text{ KNm}^{-3/2}$ . Our value

TABLE II The volume fraction of the cementite, initial interlamellar spacing and measured  $k$

	Trans. temp. (K)	$V_{\text{cem}}^a$	$\lambda_0$ ( $\mu\text{m}$ )	$k$ ( $\text{KNm}^{-3/2}$ )
Steel A	853	0.075	0.212	479.6
Steel B	853	0.098	0.168	552.2
Steel C1	923	0.120	0.222	590.4
Steel C2	883	0.120	0.175	583.1
Steel C3	853	0.120	0.142	596.1
Steel C4	823	0.120	0.125	570.9
Steel D	853	0.135	0.140	619.4

<sup>a</sup>Calculated values.

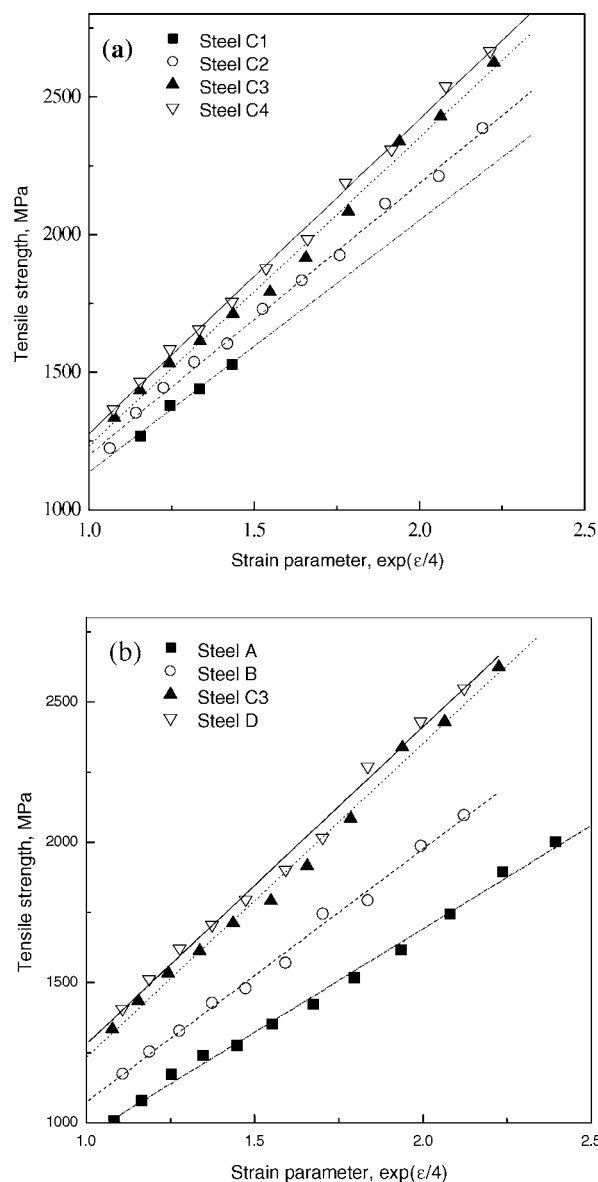


Figure 5 The plot of tensile strength with the strain parameter,  $\exp(\varepsilon/4)$ , showing (a) the effect of the interlamellar spacing and (b) the effect of the carbon content.

of  $590 \text{ KNm}^{-3/2}$  is consistent with the data for eutectoid steels measured in other investigations [3, 5]. The constancy of  $k$  in eutectoid steels indicates that the Hall-Petch parameter,  $k$ , is not influenced by the initial interlamellar spacing although the refinement of the initial interlamellar spacing increases tensile strength and hardening rate.

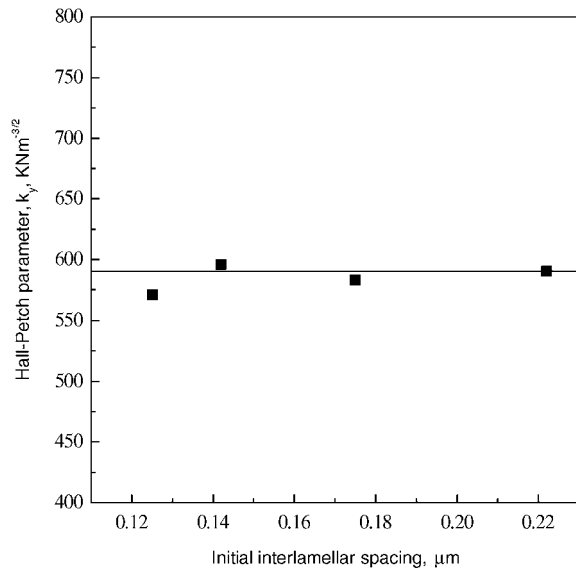


Figure 6 The variation of the Hall-Petch parameter with the interlamellar spacing in eutectoid steels.

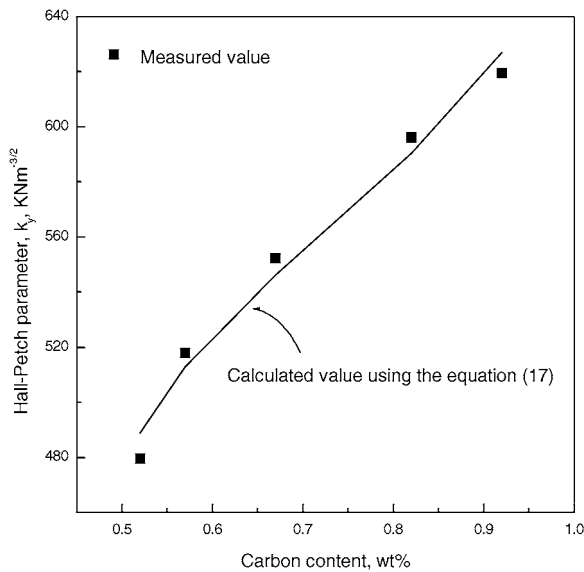


Figure 7 The variations of the calculated and measured Hall-Petch parameters as a function of the carbon content in the fully pearlitic steels.

Then, it is possible to examine qualitatively the effect of the carbon content on tensile strength, hardening rate and the Hall-Petch parameter, using the similar plot (Fig. 5b) for four steels containing the different carbon content. From the slopes shown in Fig. 5b,  $k$  can be calculated by using the Equation 2 with the values of the initial interlamellar spacing ( $\lambda_0$ ) in Table II. Fig. 7 and Table II represent the variation of the Hall-Petch parameter, which markedly increases with the carbon content. Therefore, the increase of the carbon content in pearlitic steels enhances tensile strength and hardening rate of cold drawn steels primarily by the increase of the Hall-Petch parameter as well as by reducing the initial interlamellar spacing. It is also noted that the Hall-Petch parameter,  $k$ , is not influenced by the initial interlamellar spacing, but influenced by the carbon content in cold drawn pearlitic steels. This implies that the Hall-Petch parameter can be expressed as a function of the carbon content in steels.

#### 4. Discussion

It is attempted in this study to derive a quantitative relationship between the Hall-Petch parameter and the carbon content of cold drawn fully pearlitic steels by considering a composite model. The microstructure of cold drawn pearlitic steels consists of fibrous shaped lamellar cementite and ferrite, aligned parallel to the drawing axis. Thus, the strength of cold drawn pearlitic steels can be expressed as the weighted average of the individual strength of the cementite and ferrite phases, since cementite in the pearlite serves as a load bearing component rather than a simple barrier to dislocation motion.

$$\sigma = \sigma_c V_c + \sigma_f V_f \quad (3)$$

where  $V_c$  and  $V_f$  are the fractions of the cementite and ferrite phases,  $\sigma_c$  and  $\sigma_f$  are strength of the cementite and ferrite phases, respectively. In order to apply the Equation 3 to cold drawn pearlitic steels, it is necessary to estimate individual strength of deformed cementite and ferrite phases in cold drawn pearlitic steels. However, it is not an easy task to measure experimentally the strength of heavily deformed cementite and ferrite phases. Therefore, it is reasonable to find a way to estimate strength of heavily deformed ferrite and cementite with the consideration of strengthening mechanism of those phases during wire drawing.

Meanwhile, since the lamellar cementite is plastically deformed by slip during wire drawing [13, 18, 19], it is easily expected that work hardening of the cementite phase as well as the ferrite phase contributes to the increase of strength in the drawn pearlitic steel wires. Inoue *et al.* [20] has shown that the dislocation density in cementite increases from  $10^8/\text{cm}^2$  (in annealed condition) to  $2 \times 10^{10}/\text{cm}^2$  (when heavily deformed to 92%) during cold rolling deformation. This implies that the interface of the cementite/ferrite phases would act as a barrier to the dislocation motion in a cementite lamella, as well as a generation and sink source for dislocations. If it is assumed that the strength of the deformed lamellar cementite also follows the Hall-Petch relationship, the strength of drawn pearlitic steels would be expressed as a sum of two work hardened phases.

$$\sigma = (\sigma_{c0} + k_c t_c^{-1/2}) V_c + (\sigma_{f0} + k_f t_f^{-1/2}) V_f \quad (4)$$

where  $k_c$  and  $k_f$  are the Hall-Petch constants of the lamellar cementite and ferrite,  $t_c$  and  $t_f$  are the thickness of the lamellar cementite and ferrite, respectively,  $\sigma_{c0}$  is the friction stress of the lamellar cementite and  $\sigma_{f0}$  is the friction stress of the lamellar ferrite. In the Equation 4,  $t_c$  and  $t_f$  can be expressed as functions of the interlamellar spacing and the fraction of cementite and ferrite phases. Thus, if the isostrain condition between the lamellar cementite and the lamellar ferrite during wire drawing is assumed,  $t_c$  and  $t_f$  in the Equation 4 can be expressed as;

$$\begin{aligned} t_c &= \lambda \cdot V_c \\ t_f &= \lambda - t_c = \lambda \cdot V_f \end{aligned} \quad (5)$$

By the substitution of  $t_c$  and  $t_f$  in the Equation 4 with the Equation 5,

$$\begin{aligned}\sigma &= (\sigma_{co}V_c + \sigma_{fo}V_f) + (k_c t_c^{-1/2}V_c + k_f t_f^{-1/2}V_f) \\ &= \sigma_{op} + (k_c t_c^{-1/2}V_c + k_f t_f^{-1/2}V_f) \\ &= \sigma_{op} + (k_c(\lambda \cdot V_c)^{-1/2}V_c + k_f(\lambda \cdot V_f)^{-1/2}V_f) \\ &= \sigma_{op} + (k_c \cdot V_c^{1/2} + k_f \cdot V_f^{1/2})\lambda^{-1/2}\end{aligned}\quad (6)$$

Accordingly, from the Equations of 1 and 6, the Hall-Petch constant,  $K$ , is expressed as follows;

$$K = k_c \cdot V_c^{1/2} + k_f \cdot V_f^{1/2}\quad (7)$$

Meanwhile, the flow stress of the ferrite phase in deformed pearlite can be expressed by the following equation.

$$\sigma_f = \sigma_{fo} + \alpha G b \rho^{1/2} = \sigma_{fo} + k_f \cdot t_f^{-1/2}\quad (8)$$

where  $\rho$  is the dislocation density in the lamellar ferrite and others have their usual meaning. Thus,

$$\begin{aligned}\Delta\sigma_f &= \sigma_f - \sigma_{fo} = \alpha G b \rho^{1/2} = k_f \cdot t_f^{-1/2} \\ \rho^{1/2} &= (\alpha G b)^{-1} k_f \cdot t_f^{-1/2}\end{aligned}\quad (9)$$

In the fully pearlitic steels, the interface of the cementite/ferrite has been considered as a site for generation and sink of dislocations, as well as a barrier to the dislocation motion. Thus, the characteristics of this interface would be an important factor to affect the Hall-Petch constant. According to non-pileup theory suggested by Li [21], grain boundary ledges act as dislocation sources. And the density of the ledges, which emit the dislocations, would be critical in estimating the increased dislocation density during plastic deformation. In the fully pearlitic steels with the carbon range of 0.52–0.92 wt%, the variation of the carbon content is not expected to alter characteristics of the interface, since the excessive carbon only increases the volume fraction of the lamellar cementite. Therefore, the dislocation density in the deformed lamellar ferrite would be directly influenced by the area fraction of the cementite/ferrite interface in the fully pearlitic carbon steels, if the ledge density at the cementite/ferrite interface is assumed constant in carbon steels.

According to Underwood [22], the ratio of the interface area in the fully pearlitic steels containing the different carbon content can be expressed as the ratio of the lamellar cementite volume. If the interlamellar spacing is constant,

$$S_A/S_B = V_{cA}/V_{cB}\quad (10)$$

where  $V_{cA}$  is the volume fraction of cementite in steel A,  $V_{cB}$  is that in steel B,  $S_A$  and  $S_B$  are the area fractions of the cementite/ferrite interphase in steel A and steel B, respectively. Thus, considering the relation between the dislocation density and the area fraction of

the cementite/ferrite interphase, the ratio of the dislocation density in the lamellar ferrite between steel A and steel B can be expressed as,

$$\rho_A/\rho_B \propto S_A/S_B \propto V_{cA}/V_{cB}\quad (11)$$

Since the interlamellar spacing is assumed constant, from the Equations of 9 and 11, the relationship between the Hall-Petch constant and the volume fraction of the lamellar cementite can be obtained.

$$\begin{aligned}\rho_A^{1/2}/\rho_B^{1/2} &= (k_{fA} \cdot t_{fA}^{-1/2})/(k_{fB} \cdot t_{fB}^{-1/2}) \\ &= (k_{fA} \cdot \lambda^{-1/2} \cdot V_{fA}^{-1/2})/(k_{fB} \cdot \lambda^{-1/2} \cdot V_{fB}^{-1/2}) \\ &= (k_{fA} \cdot V_{fA}^{-1/2})/(k_{fB} \cdot V_{fB}^{-1/2}) \\ &\propto V_{cA}^{1/2}/V_{cB}^{1/2}\end{aligned}\quad (12)$$

Therefore,

$$\begin{aligned}(k_{fA} \cdot V_{fA}^{-1/2})/(k_{fB} \cdot V_{fB}^{-1/2}) &\propto V_{cA}^{1/2}/V_{cB}^{1/2} \\ k_{fA} &\propto (V_{cA}^{1/2} V_{fA}^{1/2}) \\ k_{fB} &\propto (V_{cB}^{1/2} V_{fB}^{1/2})\end{aligned}\quad (13)$$

Among several microstructural features in fully pearlitic carbon steels, the interlamellar spacing does not affect the Hall-Petch constant as mentioned before, and other microstructural features except for the volume fraction of the lamellar cementite and ferrite do not seem to have an influence on the dislocation density. Accordingly, the Hall-Petch constant of the lamellar ferrite,  $k_f$ , can be expressed as a function of the volume fraction of the lamellar cementite and ferrite.

$$k_f = C_1 V_c^{1/2} V_f^{1/2}\quad (14)$$

where  $C_1$  is the constant. Therefore, the Hall-Petch constant in the Equation 7,  $K$ , can be rewritten as

$$K = k_c \cdot V_c^{1/2} + C_1 V_c^{1/2} \cdot V_f\quad (15)$$

In spite of the contribution of the lamellar cementite in the Equation 15, the actual contribution of the lamellar cementite to the strengthening seems to be less than expected in cold drawn pearlitic steels. Earlier investigations have reported that the lamellar cementite in the fine pearlite as well as in the coarse pearlite is fragmented at the extremely high drawing strain [23, 24]. However, tensile strength of cold drawn pearlitic steel wires increases steadily even at the high strain region, where the lamellar cementite is fragmented. This implies that the strengthening of the deformed lamellar ferrite would be the main strengthening mechanism in the heavily deformed pearlite, and the contribution of the strengthening of the deformed lamellar cementite would be much smaller than that of the deformed lamellar ferrite in the heavily deformed pearlite. Thus, since  $k_c \cdot V_c^{1/2} \ll k_f \cdot V_f^{1/2}$ , the Hall-Petch constant,  $K$ , can be expressed as a function of the volume fraction of the

cementite, i.e., the carbon content.

$$K \approx C_1 V_c^{1/2} \cdot (1 - V_c) \quad (16)$$

where  $V_c$  is expressed as  $[(W_{cem}/\rho_{cem})/(W_{cem}/\rho_{cem} + W_{fer}/\rho_{fer})]$ , with  $\rho_{cem}$  and  $\rho_{fer}$  as the density of cementite (7.20 gr/cm<sup>3</sup>) and ferrite (7.87 gr/cm<sup>3</sup>),  $W_{cem}$  and  $W_{fer}$  as the weight fractions of cementite and ferrite.

As mentioned earlier, since the magnitude of the Hall-Petch parameter,  $k$ , is equivalent to  $\sqrt{2}$  times the Hall-Petch constant,  $K$ ,  $k$  can be calculated from the Equation 16 using the constant  $C'$  instead of  $C_1$ . From the linear regression of measured  $k$  in Table II with  $V_c^{1/2} \cdot (1 - V_c)$ , the Hall-Petch parameter can be expressed as a function of the volume fraction of cementite, i.e. the carbon content.

$$k = C' \cdot V_c^{1/2} \cdot (1 - V_c) \quad (17)$$

where  $C'$  is found to be 1973 KNm<sup>-3/2</sup> in this study. The calculated values of  $k$  using the Equation 17 are compared with the measured values in Fig. 7. The good agreement is found between experimental and calculated values of  $k$ , which evidences that the Hall-Petch parameter is influenced by the volume fraction of the lamellar cementite, i.e. the carbon content. In addition, work hardening of pearlitic steels during wire drawing significantly depends on work hardening of the lamellar ferrite that is also influenced by the carbon content.

## 5. Conclusions

In this study, it is attempted to investigate the variation of the Hall-Petch parameter,  $k$ , with the carbon content in cold drawn pearlitic steels, and to establish a quantitative relationship between  $k$  and the carbon content. The morphology of cementite in the pearlite changes from a type of continuous plates into discrete ones with the reduction of carbon content in the pearlite region. However, the microstructures in cold drawn fully pearlitic steels with the drawing strain above 2.0 consist of all the fibrous shaped cementite and ferrite lamellae aligned along the drawing axis.

The increase of the carbon content in pearlitic steels raises tensile strength and hardening rate,  $k/(2\lambda_0)^{1/2}$ , of cold drawn steels by the refinement of the initial interlamellar spacing and the increase of the Hall-Petch parameter. The Hall-Petch parameter,  $k$ , is not influenced by the initial interlamellar spacing although the

refinement of the initial interlamellar spacing increases tensile strength and hardening rate during wire drawing. However, the carbon content in cold drawn pearlitic steels significantly affects the magnitude of the Hall-Petch parameter. In addition, the magnitude of the Hall-Petch parameter,  $k$ , is suggested as a function of the volume fraction of cementite, i.e. the carbon content,  $k = \text{constant} \cdot V_c^{1/2} \cdot (1 - V_c)$ . This relationship shows the good agreement between experimental and calculated values.

## References

1. E. O. HALL, *Proc. Phys. Soc.* **B64** (1951) 747.
2. N. J. PETCH, *J. Iron Steel Inst.* **174** (1953) 25.
3. J. D. EMBURY and R. M. FISHER, *Acta Met.* **14** (1966) 147.
4. G. LANGFORD, *Met. Trans. A* **8A** (1977) 861.
5. I. P. KEMP, *Mat. Forums* **14** (1990) 270.
6. B. MINTS, *Metals Tech.* **11** (1984) 265.
7. M. DOLLAR, I. M. BERNSTEIN and A. W. THOMPSON, *Acta Metall.* **36** (1988) 311.
8. H. CHOI and K. PARK, *Scripta Mater.* **34** (1996) 857.
9. D. CHEETHAM and N. RIDLEY, *Metal Sci.* **9** (1975) 422.
10. Y. OHMORI and R. W. K. HONEYCOMBE, in Proceedings International Conference of Sci. Technol. Iron Steel, section 6, Tokyo (1971) p. 1160.
11. J. J. PEPE, *Met. Trans.* **4A** (1973) 2455.
12. M. A. P. DEWEY and G. W. BRIERS, *J. Iron Steel Inst.* **204** (1966) 102.
13. D. A. PORTER, K. E. EASTERING and G. D. W. SMITH, *Acta Met.* **26** (1978) 1405.
14. E. C. PURCINO and P. R. CETLIN, *Scripta Met.* **25** (1991) 167.
15. V. K. CHANDHOK, A. KASAK and J. P. HIRTH, *Trans. ASM* **59** (1966) 288.
16. L. E. MILLER and G. C. SMITH, *J. Iron Steel Inst.* **208** (1970) 998.
17. D. J. ALEXANDER and I. M. BERNSTEIN, in "Phase Transformations in Ferrous Alloys," edited by A. R. Marder and J. I. Goldstein (TMS/AIME, Warrendale, PA, 1984) p. 243.
18. J. G. SEVILLANO, *Mater. Sci. and Eng.* **21** (1975) 221.
19. K. MAURER and D. H. WARRINGTON, *Phil. Mag.* **15** (1967) 321.
20. A. INOUE, T. OGURA and T. MASUMOTO, *Trans. JIM* **17** (1976) 149.
21. J. C. M. LI, *Trans. AIME* **227** (1963) 239.
22. E. E. UNDERWOOD, in "Quantitative Stereology" (Addison-Wesley, Massachusetts, 1969) p. 73.
23. J. LANGUILLAUME, G. KAPELSKI and B. BAUDELET, *Acta Mater.* **45** (1997) 1201.
24. H. G. READ, W. T. REYNOLDS JR., K. HONO and T. TARUI, *Scripta Mater.* **37** (1997) 1221.

Received 20 September 2001  
and accepted 30 January 2002